Catalysis Science & Technology

ROYAL SOCIETY OF CHEMISTRY

www.rsc.org/catalysis

Hydrodeoxygenation of Microalgae Oil to Green Diesel over Pt, Rh and Presulfided NiMo Catalysts

Lin Zhou* and Adeniyi Lawal

New Jersey Center for Microchemical Systems, Dept. of Chemical Engineering and Materials Science, Stevens Institute of Technology, 1 Castle Point on Hudson, Hoboken, NJ 07030, USA

Keywords:

Hydrodeoxygenation (HDO)

Microalgae oil

Coke formation

Methane formation

Hydrogen consumption

*Corresponding author,

Tel.; +1 201 216 8314; Fax: +1 201 216 8306; Email: lzhou4@stevens.edu

Abstract

The catalytic characteristics, activity and selectivity of 1% Pt/Al_2O_3, 0.5% Rh/Al_2O_3 and presulfided NiMo/Al_2O_3 catalysts have been investigated in hydrodeoxygenation of microalgae (Nannochloropsis salina) oil to produce green diesel in a microreactor. Coke accumulation decreased in the order NiMo > Pt > Rh. The amount of formed coke over NiMo increased with reaction duration, while no on-stream time dependence was found over Pt and Rh. Rhodium was found to be very active for CH_4 production via hydrocracking at its fresh reduced state. The activity and selectivity of all three investigated catalysts were positively affected by increased reaction pressure, temperature, H_2/Oil ratio and residence time. The selectivity of NiMo for hydrodehydration (DHYD) route was changed to Hydrodecarbonylation/Hydrodecarboxylation (DCO/DCO2) route at reduced H_2/Oil ratio and residence time, while the selectivity of Pt and Rh for DCO/DCO2 route was not affected by reaction conditions. The highest hydrocarbon yield, 76.5%, was obtained over 1% Pt (310^{o}C, 500 psig, 1000 SmL/mL gas/oil ratio, 1.5s residence time), which is 13.8% higher than that over NiMo (360^{o}C, 500 psig, 1000 SmL/mL gas/oil ratio, 1s residence time). The 50^{o}C decrease in reaction temperature for Pt indicates a possible energy saving via heat supply.

1. Introduction

Over the next few decades, as economies expand and evolve, the global energy demand for transportation is expected to continue to grow significantly. It is estimated that global demand for energy for commercial transportation will rise by 70 percent from 2010 to 2040. Due to its affordability, availability, portability and high energy density, liquid fuel, including gasoline, diesel, jet fuel and fuel oil, will remain the energy of choice for most types of transportation. Seventy-five percent of the heavy-duty transportation energy requirements are met by diesel fuel, due to its widespread availability and the robust ability of diesel engine technology to handle heavy loads. With an estimate of about 80 percent growth in heavy-duty transportation fuel requirements, demand for diesel is expected to grow sharply by about 75 percent from 2010 to 2040 [1]. Petroleum diesel is refined from crude oil, and approximately 12 gallons of diesel fuel can be produced from each 42-gallon barrel of crude oil [2]. The CO_2 emissions from diesel can be calculated based on its carbon content, 2,778 g per gallon diesel, which is 10,084 g CO_2 per gallon diesel [3]. Therefore, the combination of continued crude oil depletion, the ever-growing need for renewable energy resource, and the CO_2 emission problem, are a motivation for research and development into advanced biofuels.

It has been reported that the oleaginous feedstock, the main components of which are triglycerides and free fatty acids, has higher energy content than the lignocellulose[4]. Microalgae, as a source of oleaginous feedstock for green diesel production is currently attracting attention of researchers. Green diesel, produced from hydrotreating of triglycerides, is chemically similar to petroleum diesel with excellent stability and cold-flow properties, and can be blended with petroleum diesel in any proportion. It can be transported in existing infrastructure and used in diesel engines without any modification. Microalgae, which provide the route for collection, conversion and storage of solar energy in the form of oxygenated hydrocarbon compounds, have been considered as potential candidate for fuel production [5]. The utilization of microalgae for green diesel production will not compromise the food and oil production from land crops. Energy is captured by microalgae through CO_2 fixation by photosynthesis, which will help to maintain and improve the air quality. Moreover, because the nutrients in wastewater (especially nitrogen and phosphorus) could be exploited by algae growth, the algae cultivation can also be coupled with wastewater treatment [5].

The sulfur, nitrogen, and phosphorus contents in microalgae oil are relatively low, and the main heteroatom needed to be removed to produce green diesel is oxygen. Triglycerides constitute the major component (> 80%) in algae oil, and due to the nature of oxygen bonding in triglycerides, oxygen is proposed to be removed by adding hydrogen, hydrodeoxygenation (HDO), which occurs through two routes: (1) Hydrodehydration (DHYD), in which oxygen is removed in the form of H_2O, and (2) Hydrodecarboxylation (DCO2) or Hydrodecarbonylation (DCO), in which oxygen is removed in the form of CO_2 and CO respectively [6].

Catalyst selection is crucial in the hydrotreating step, due to its role in controlling the yield and selectivity to different products, which in turn impact both capital and operating costs. Because the oxygen content in crude oil is at rather low levels, on the order of 0.5%, not much concern is given to HDO in petroleum refining. Therefore, no hydrotreating catalysts have been specially formulated for HDO of oleaginous feedstock with much higher oxygen content than crude oil. Thus, one of the critical challenges posed by HDO of algae oils is the development of specific catalysts to make the process economical.

Compared to the non-selective acidic catalysts, which give a broad distribution of hydrocarbons, the supported metal catalysts in reduced or sulfided state, are more commonly used in industry because they produce a narrow range of hydrocarbons [7]. In conventional petroleum refining, the transition metal sulfides, Mo or W, promoted with Co or Ni metal sulfides have been utilized in hydrotreating units to remove sulfur (hydrodesulfurization, HDS), nitrogen (hydrodenitrogenation, HDN), metals (hydrodemetalation, HDM) and oxygen (hydrodeoxygenation, HDO) from the heavy gas oil feedstock [4]. These conventional hydrotreating catalysts have been studied in the HDO process [8-14]. The sulfided NiMo catalyst is found to be more active than sulfided CoMo catalyst in hydrotreating of oxygen-containing compounds, such as fatty acid methyl ester (FAME) [15, 16]. However, it has been reported that the leaching of sulfur from the sulfided catalyst surface will cause the deactivation of the catalyst and contaminate the product [7, 17-19]. Water produced from DHYD has been found to accelerate the sulfur leaching, and decrease the activity and thus affect the selectivity of both sulfided NiMo and CoMo catalysts [16]. Moreover, the conventional hydrotreating catalyst was found to prefer the DHYD route, which requires a higher H_2 consumption to produce hydrocarbons.

Supported noble metal-based catalysts have been investigated in reduced state, with Palladium (Pd) being the most studied [20]. The Pd-based catalyst was found to prefer the DCO2 route, which does not require a stoichiometric level of H2 consumption to produce renewable diesel. The best catalytic performance was obtained from a commercial Pd/C catalyst in HDO of stearic acid in a continuous reactor at 360^{o}C. The conversion of steric acid after 92 h (5500 min) time-on-stream was about 40%, although it was90% at the beginning of the experiment [21]. The rapid deactivation of Pd/C catalyst was also reported in HDO of lauric acid at 255-300^{o}C [21]. The deactivation of Pd/C catalyst was caused by a combination of coking, and poisoning by the produced gases, mainly CO and CO_2 [21]. Other supported precious metal catalysts, including Pt, Rh, Ru and Ir, have also been studied mostly for the HDO of model compounds, such as stearic acid, ethyl stearate and tristearine, in batch or semi-batch reactors [22-24]. Lack of experimental data on the performance of replacement catalysts for sulfided NiMo, especially the precious metal-based catalysts, for HDO of actual algae oil feedstock in a continuous flow reactor is one of the key technical challenges that need to be addressed.

In the present study, the hydrodeoxygenation of microalgae oil extracted from Nannochloropsis salina strain, the workhorse of the algae industry, was conducted in a microreactor with excellent mass transfer characteristics. There is a dearth of experimental data in the literature on hydrodeoxygenation of microalgae oil, and our overall goal was to contribute reliable data that can be used in pilot studies in a prelude to industrial scale-up. In relation to that, microreactors provide ease of scale-up through the numbering-up approach, which have been demonstrated elsewhere [14, 25-30]. Three catalysts, 1% Pt/Al_2O_3, 0.5% Rh/Al_2O_3 and presulfided $NiMo/Al_2O_3$, were investigated in terms of their catalytic characteristics, activity and selectivity by analyzing the gas and liquid product. Comparison of their performance will guide further catalyst formulation and process scale-up and optimization.

2. Experimental Section

2.1 Materials

Reactants

Hydrogen (5.0 grade, ultra-high purity), Nitrogen (5.0 grade, ultra-high purity), and Air (5.0 grade, ultra-high purity) were all purchased from Praxair.

In order to make the microalgae oil to green diesel process commercially feasible, the investment required by all aspects of the product chain need to be taken into consideration. Due to its high lipids content (up to 70% of dry weight), and relatively high biomass yield, microalgae oil extracted from Nannochloropsis salina, and provided to us by Valicor Renewables, LLC Inc., was used in this present work. Unlike vegetable oils which are essentially 100% acylglycerides, only 47.45% of the Nannochloropsis salina oil was identified to be acylglycerides and free fatty acids, with the remainder categorized as unidentified portion. The quantification results can be found elsewhere [14], and the corresponding fatty acid (FA) profile as determined by Valicor is given in Table 1. The algae oil is in semisolid form at room temperature, therefore, solvent is needed to process the oil in a continuous reactor. One gram of algae oil was dissolved in 100mL of n-dodecane (99+ %, Alfa Aesar) to make 1.3wt% solution, and the solution was vacuum-filtered through the 410 filter paper (VWR, 1 μm retention) to remove any residual particles (>10wt% of the oil) before feeding into the reactor. Although the potential of blockage to the reactor system is low for an industrial reactor, residual particles that accumulate over a period of time and are adsorbed on the catalyst surface can block the active sites or the pores of the catalyst, which will reduce the apparent catalyst activity and result in low system productivity. It should also be mentioned that, based on our experience with microalgae oil extracted from other algae species, such as Chlorella, which has negligible residual solid content and flows freely at room temperature, the solvent and vacuum-filtration pretreatment process may not be needed. However, for industrial implementation of our current process, the dodecane can be replaced by the middle distillates from refinery, such as the light atmospheric gas oil (LAGO), and will not affect the process economics significantly. The compatibility of all process equipment and pipelines, with the properties of algae oil, especially the corrosive properties, needs to be considered when processing pure algae oil, as constraints imposed by material selection can increase both the capital and operating investment. The cost of vacuum-filtration is negligible in comparison to the cost of algae oil production, which comprises mainly algae cultivation and oil extraction. This is the cost that determines the economic feasibility of the whole biofuel production process. Therefore, the co-processing of Nannochloropsis salina algae oil with solvent after vacuum-filtration is proposed as our current process for green diesel production. .

Table 1 ***Fatty Acid Profile of Microalgae Oil***[a]**.**

Fatty Acid Profile (wt %)									
$C_{14:0}$[b]	$C_{14:1}$	$C_{16:0}$	$C_{16:1n7}$	$C_{18:0}$	$C_{18:1}$-*cis*	$C_{18:1}$-trans	$C_{18:2}$	$C_{18:3}$	$C_{20:0}$
2.19	0.04	12.21	15.91	0.41	3.05	1.10	0.96	0.04	0.06
$C_{20:1}$	$C_{20:2n6}$	$C_{20:4n6}$	$C_{20:3n3}$	$C_{20:5n3}$	$C_{22:0}$	$C_{21:5n3}$	C_{24}	$C_{24:1}$	other
0.03	0.38	1.43	3.52	7.66	0.07	0.05	0.10	0.05	0.04

[a] Microalgae oil is extracted from Nannochloropsis salina and provided by Valicor Renewables, LLC Inc.

[b] The nomenclature shows the number of carbon atoms, the number of C=C double bonds, and the position of the C=C double bond.

Catalyst

The NiMo/γ-Al_2O_3 catalyst was provided by Albemarle (presulfided and supplied by Eurecat, U.S.A.) Houston, TX. A typical composition of this commercial hydrotreating catalyst is 4.03% NiO and 13.20% MoO_3 on dry basis [31].

Commercial catalysts, 1% Pt and 0.5% Rh, were purchased from Alfa Aesar, a Johnson Matthey company. The two catalysts were all supported on 2.7-3.3mm γ-Al_2O_3 pellets, and were ground and sieved to 75-150 μm particle size fraction before packing into the reactor. Previous studies [25-27, 29, 30] have revealed that the internal diffusion has negligible influence on the reaction rate for this catalyst particle size range. The two catalysts have the same bulk density, and the molar mass of Rh (102.90 g/mol) is nearly half of that of Pt (195.09 g/mol). Therefore, the number of Pt atoms is the same as that of Rh for the same volume of catalyst.

2.2. Experimental Setup and Procedure

As shown in Scheme 1, the hydrodeoxygenation of microalgae oil was conducted in a continuous flow microreactor, the inner diameter of which was 0.762mm. All three investigated catalysts were ground and sieved to 75-150 μm before being packed in the reactor. At the entrance and exit of the reactor, a 1/8 inch outer diameter tube was connected to the reactor and it was packed with glass beads of 90 μm. To retain the packed particles in each tube section, Hastelloy micron fitter-cloth (200 × 1150 meshes, Unique Wire Weaving Co., Hillside, NJ) was placed inside each union between the 1/8 inch tube and reactor. The reactor was placed in an electric furnace with digital temperature control and readout, and the temperature of the furnace was also measured by a hand-held temperature meter for confirmation. Pressure at the entrance and exit of the reactor was measured by two pressure transmitters. System pressure was adjusted by a back pressure regulator (BPR) installed downstream. Gas flow was regulated by a mass flow controller (sccm, standard cubic centimeter per minute), which was calibrated by an Agilent ADM 2000 Universal gas flowmeter routinely. According to previous studies, introduction of gas and liquid flows head to head generates a short slug length which enhances mixing in two-phase flows [28], therefore, liquid feed pumped by a HPLC pump (mL/min) first contacted the gas flow at a T-mixer before entering the reactor. Due to the low product flow rate, a sample loop was connected between the reactor exit and the BPR, and liquid product was collected every hour at ambient conditions for off-line analysis. The remaining product stream continued to the gas-liquid separator, where the liquid condensed and gas proceeded through an inline filter to the GC-TCD for analysis.

In-situ reduction of fresh catalysts was done with pure hydrogen flow at 310°C and 500 psig for 2 hours before starting any reaction run. In a microreactor, it was difficult to recover the used catalyst and clean it with solvent. In order to remove any liquid or solid residues from the catalyst that may affect the coke formation result, the system was purged with compressed nitrogen. Therefore, the "coke" mentioned in section 3.1 was referred to as all carbonaceous residues that cannot be removed through nitrogen purging. For gas product analysis (sections 3.2 and 3.3), nitrogen which was fed into the system in a mixture with reactant hydrogen, was used as internal standard. The composition of the nitrogen/hydrogen mixture was also confirmed by GC-TCD before starting each reaction.

2.3. Product Analysis

Liquid Product

As shown in Table 1, the C14, C16, C18, and C20 fatty acids are the main components in microalgae (Nannochloropsis salina) oil fatty acid profile. According to the HDO mechanism mentioned above, the diesel range alkanes, C13 to C20 hydrocarbons, were the focus of this study. To identify the components in the liquid product and quantify them, the liquid product was directly injected by a CP-8400 Autosampler to the Varian 450 Gas Chromatograph (GC) equipped with a flame ionization detector (FID) under the conditions stated below:

Column: ZB-1HT nonpolar capillary column (30 m × 0.25 mm × 0.25 μm)

Oven: 50°C (1min), 15°C/min to 240°C (5min)

Injector: 250°C

Detector: FID, 280°C

Carrier gas: Helium

Injection: 1μ, 1:20 split

Before analyzing each batch of samples, GC external calibration was done with 4 standards containing C13-C20 hydrocarbons of different concentrations to get the response factor and retention time of each hydrocarbon. The C13-C20 hydrocarbon yield was used to evaluate the catalyst activity, and was calculated based on the quantified FA (47.45%) in the liquid feed.

$$C13-C20\ Hydrocarbon\ Yield\ (\%) = \frac{total\ mass\ of\ C13{-}C20\ hydrocarbon\ in\ product}{total\ mass\ of\ FA\ in\ liqud\ feed} \times 100 \qquad (1)$$

The Even-numbered carbon hydrocarbon to odd-numbered carbon hydrocarbon ratio (HC(2n)/HC(2n-1)) is a reflection of catalyst selectivity, and is defined as

$$HC(2n)/HC(2n-1) = \frac{mass\ of\ even{-}numbered\ carbon\ hydrocarbon\ in\ product}{mass\ of\ odd{-}numbered\ carbon\ hydrocarbon\ in\ product} \qquad (2)$$

Space-time yield (STY) indicates the rate of hydrocarbon formation, and is defined as

$$STY_{hydrocarbon} = \frac{mass\ of\ hydrocarbon\ produced/time}{mass\ of\ catalyst} \qquad (3)$$

Gas Product Analysis

To study the coke formation (section 3.1), methane formation (section 3.2) and hydrogen consumption (section 3.3), quantification of H_2, N_2, CH_4, and CO_2 was of vital importance. Gas sample was injected into the Shimadzu GC-14B through a 10-port sampling valve and analyzed by a thermal conductivity detector (TCD). The sample eluted by Argon (Ar) first flowed through the HP-PLOT Q column and then the HP-Molseive column. The temperature program in the column oven was: initially held at 60^{o}C for 13.5 min, then ramped at 25^{o}C/min to 160^{o}C and held for 6.5 min. After each experiment, GC was baked at 220 ^{o}C for 4 hours to get rid of any liquid residue from the flow system. In the coke formation determination, pure air was fed into the system, and the nitrogen contained therein was used as internal standard to quantify the CO_2 production. In the methane formation and hydrogen consumption study, the added nitrogen (1sccm, 20 mol%) was used as internal standard to account for the gas flow rate change during the reaction.

3. Results and Discussion

3.1. Analysis of External Mass Transfer Limitation

In the present study, all the catalyst evaluation experiments were performed in the Taylor flow regime, comprising of alternating liquid slugs and gas bubbles. For this heterogeneous reaction of microalgae oil with hydrogen on the γ-alumina supported catalyst, the main external mass transfer resistances occur at the gas-liquid and liquid-solid interfaces, with the former being predominant. The mass transfer rates through interfaces depend greatly on flow velocity; therefore, the overall external mass transfer limitation can be investigated experimentally by studying the change of hydrocarbon yield rate at different superficial flow velocities. The other process conditions, including reactor ID, gas to oil ratio, residence time and reaction temperature and pressure, need to be kept the same for all experiments, with the constant residence time being achieved by varying the reactor length, in other words the amount of catalyst. Figure 1 shows that the STY of C13 to C20 hydrocarbon is independent of the superficial flow velocity within the studied range. This indicates the absence of external mass transfer limitation beyond a velocity of 0.117 m/s, which was chosen as the baseline velocity for all subsequent performance studies. The same non-external mass transfer controlled flow velocity range has also been reported with respect to presulfided NiMo catalyst [14]. Since the external mass transfer is not catalyst species dependent, the flow velocity range without external mass transfer limitation is expected to be the same for Rh catalyst, and the performance studies over Rh catalyst was also conducted in the same range.

3.2. Analysis of Internal Mass Transfer Limitation.

Internal mass transfer refers to the diffusion of reactants from the catalyst pellet pore entrance into the pore. Reactions are limited by internal mass transfer when there is a concentration gradient within the catalyst, with the concentration inside the pores much lower than that at the entrance. In order to account for variations in concentration throughout the catalyst pellet, the Weisz-Prater parameter (C_{wp}) is introduced [32].

$$C_{wp} = \frac{actual\ reaction\ rate}{a\ diffusion\ rate} = \frac{-r'_{A(obs)}\rho_P R^2}{D_e C_{As}} \tag{4}$$

Where

$-r'_{A(obs)}$: Observed reaction rate, 9.22 × 10^{-5} g hydrocarbon/ g cat. /s.

ρ_P: Density of catalyst pellets, 0.29 g cat. /cm^3.

R: Characteristic diameter of the catalyst pellets, 112.5×10^{-4} cm.

C_{AS}: Hydrogen concentration at the external surface of the catalyst pellets, which is the hydrogen solubility in dodecane approximately, 360 g/m^3.

D_e: Effective diffusivity of hydrogen in the catalyst pellets, $D_e=(D_{AB}\phi_P\sigma_C)/\tau$, where D_{AB}: Binary diffusivity of hydrogen in dodecane, 1.12×10^{-7} m^2/s [33]; ϕ_P: Porosity of the catalyst pellets, 0.4-0.6; σ_C:Catalyst constriction factor,0.7-0.8 ; τ: catalyst tortuosity, 2-8 [32]. Then, the D_e is calculated to be between 2.69×10^{-8} and 3.92×10^{-9} m^2/s.

Based on the ranges of the catalyst porosity, constriction factor, and tortuosity, the calculated Weisz-Prater parameter was between 0.240 and 0.035. According to the Weisz-Prater criterion, $C_{WP} \ll 1$ means there is no concentration gradient within the pellet, and consequently no diffusion limitations existed in our experiments.

3.3 Coke formation

In the HDO of microalgae oil, the carbon lost to the gas phase, including CO, CO_2, CH_4 and light hydrocarbons, and solid phase, mainly coke, will affect the carbon recovery in the liquid product. Moreover, coke formation during the catalytic upgrading of carbon-rich feedstock is one of the major causes of catalyst deactivation. Therefore, the extent of coke formation in HDO of microalgae oil over Pt, Rh, and NiMo was firstly studied. The definition of what constitutes coke in liquid-phase reactions, especially for liquids with high boiling point, depends on the coke quantification method, and is quite different from that in gas-phase reactions [34]. In the present study, coke is referred to as all carbonaceous residues that cannot be removed through purging by gas (N_2).

In order to investigate coke accumulation with time-on-stream, HDO of microalgae oil was conducted for 10 h, 20 h, and 30 h using Pt, Rh and NiMo under the same process conditions, starting each experimental run with reduced fresh catalysts. Upon the completion of HDO reaction, the reactor system was purged with nitrogen to get rid of any remaining oil from the catalyst surface. Because it is difficult to directly quantify the formed coke accurately in a microreactor, alternatively, the amount of coke can be determined through coke burn-off (oxidization). The concentration (mol %) of produced CO_2 in the combustion product gas is an indication of the extent of coke formation during the HDO reaction. The trend of coke formation during different reaction periods over 3 catalysts is depicted in Figure 2, with the slope of each trend line representing the coke formation rate. Under the experimental conditions, the coke formation decreased in the following order for all studied HDO reaction time-on-stream: NiMo > 1% Pt > 0.5% Rh. The amount of coke accumulated on the presulfided NiMo catalyst increased with HDO time-on-stream; while no time dependence of coke accumulation was observed on Pt- and Rh-based catalysts. This Pt result is in agreement with previous studies on hydrogenation of vegetable oils conducted in a batch reactor using a different coke quantification method, and which reported that the formation of coke precursors on Pt was very slow [34].The amount of coke formed and the rate of formation of coke for NiMo are always much higher than the values for the two precious metal catalysts studied, therefore, the carbon lost is more for NiMo than for Pt and Rh. However, because dilute algae oil solution (1.32 wt %) was used in this study, the actual amount of coke deposit was small, and no obvious reduction in C13 to C20 hydrocarbon yield was observed over 30 hours of reaction It should be noted that, in industrial practice, although significantly larger amount of catalyst will be used to process higher algae oil concentration feedstock, the accumulation of coke deposit with reaction time on NiMo catalyst may lead to gradual catalyst deactivation. This will result in the decrease in oxygen removal efficiency as well as the carbon recovery. In addition, more frequent regeneration process will be required by NiMo to restore the catalyst activity and selectivity, in comparison to the precious metal based catalyst.

3.4 Methane Formation

Methane is known to be produced through methanation ($CO + 3H_2 \rightarrow CH_4 + H_2O$) and hydrocracking in the HDO process. In addition to the reduction of carbon recovery in liquid phase, the formation of gaseous product will also negatively affect the hydrogen partial pressure, which has been reported to potentially reduce catalyst activity [35]. Moreover, the formation of light hydrocarbons, especially CH_4, of which the H/C ratio is the highest for all hydrocarbons, will increase the hydrogen consumption, and consequently render the whole upgrading process less economically effective. It is noteworthy that the reduction in the formation of methane, which is one of the greenhouse gases (GHG) with a global warming potential (GWP) 23 times higher than that of CO2, will significantly provide environmental benefits [36].

The yield of CH_4 per gram algae oil processed over 3 catalysts is depicted in Figure 3. NiMo showed the lowest activity for CH_4 formation, and no CH_4 was detected in the product gas. Precious metal based catalyst showed high activity in CH_4 production initially, which quickly decreased with reaction time-on-stream. A similar result had been reported in a study of Pt [37]. For the first 7 h, Rh was much more active than Pt in producing CH_4, but less active after 7 h. After 16 h, there was no CH_4 detectable in the Rh product gas. It should be also noted that, during the first 5 hours of reaction over Rh, the CH_4 yield was much higher than the maximum theoretical CH_4 production through methanation from CO, which indicated that the CH_4 was mainly formed through hydrocracking. The analysis of liquid product showed that more cracking product, i.e., hydrocarbons that contain less than 12 carbons, was found in the Rh product, but decreased with time, which validated the hydrocracking activity of fresh reduced Rh catalyst. By examining the trend in the change of CH_4 formation with reaction time, it is expected that the amount of produced methane will stabilize below the detection limit of GC-TCD over all three catalysts, but longer time is needed to reach the stability when using Pt. Therefore, in industrial practice, where the catalyst life is expected to be much longer than 30 hours (typically >24 months), the methane formation will not be much of a concern in the HDO of algae oil for all three studied catalysts.

3.5. Hydrogen consumption

Hydrogen consumption based on per gram algae oil processed over NiMo, Pt and Rh catalyst has been investigated experimentally, and the results are shown in Figure 4. Hydrogen consumption follows the same trend as CH_4 formation over Rh up to 7 hours (Figure 3). For 1 mol of CH_4 produced, 3 moles of H_2 will be consumed through methanation of CO, while only 1 mole H_2 is demanded through hydrocracking. However, the H_2 consumption over Rh was not shown to be 3 times that of the formed CH_4. Therefore, it again confirms that the Rh was initially very active for hydrocracking to produce CH_4. After 16 h, the H_2 consumption over Rh stabilized around $24x10^{-3}$ mol H_2/g AO. For the NiMo and Pt catalyst, the H_2 consumption increased with time initially and stabilized around $40x10^{-3}$ mol H_2/g AO and $30x10^{-3}$ mol H_2/g AO respectively. It should be noted that the CH_4 formation over Pt was mainly through hydrocracking initially, which consumed less hydrogen than the HDO reaction. The stabilized H_2 consumption over Pt is slightly higher than that over Rh due to its slightly higher production of CH_4 mainly through methanation. NiMo consumed much more H_2 than Pt and Rh, because more H_2 is demanded in

DHYD route, which is favored by NiMo, than in DCO route, the path favored by Pt and Rh. Therefore, due to the difference in selectivity, precious metal catalysts consume less hydrogen in removing the same amount of oxygen, though 1 mole carbon will be sacrificed in the form of CO, CO_2 and CH_4 lost into the gas phase for every 2 moles of hydrogen saved.

As previously reported [14], the content of fatty acids, including Monoacylglycerides (MAG), Diacylglycerides (DAG), Triacylglycerides (TAG) and free fatty acids (FFA) in Nannochloropsis salina is 47.45 wt %, and the corresponding fatty acid profile is given in Table 1. The mechanism of HDO of FA has been fully illustrated and the detailed reaction pathway has been provided elsewhere [6, 38]. Based on the reaction pathways, the hydrogen demand for each step of reaction is listed in Table 2. The oxygen removal through hydrodehydration route involves reactions 1, 2, 3, 4, and 5, while that through the hydrodecarbonylation route involves reactions 1, 2, 3, and 6. In conjunction with the fatty acid profile in Table 1, the theoretical amounts of H_2 required to remove oxygen from only the acylglycerides and free fatty acids portion of algae oil through DHYD and DCO route were calculated to be 9.5×10^{-3} mol H_2/g AO, and 4.3×10^{-3} mol H_2/g AO respectively. However, the measured stabilized hydrogen consumption amounts over NiMo and precious metal based catalysts were higher than twice the theoretically calculated values. Therefore, the oxygen removal from the unidentified portion of algae oil consumed much more hydrogen than the identified acylglycerides and free fatty acids portion. However, the oxygen content and degree of unsaturation are only slightly higher in the latter [14]. It indicates that the HDO mechanism of the unidentified portion of Nannochloropsis salina oil is different from that of the acylglycerides.

Table 2. ***Hydrogen Demand in Hydrodeoxygenation of Acylglycerides and Free Fatty Acids.***

Reaction	Hydrogen consumption per mole FA chain (mol H_2/mol FA)
1. Saturation of C=C double bond	1 mol H_2 demanded for per mol double bond
2. Hydrogenolysis to produce FFA	1
3. FFA → R-CHO (Fatty aldehyde)	1
4. R-CHO → R-CH_2OH (Fatty alcohol)	1
5. R-CH_2OH → HC(2n)	1
6. R-CHO → HC(2n-1)	0

3.6. Effect of Reaction Pressure

In order to study the effect of reaction pressure on catalyst activity and selectivity, experiments were conducted in the pressure range of 300 to 500 psig. Other process parameters, including reaction temperature, H_2/Oil ratio, fluid flow rates and weight hourly space velocity (WHSV) were kept the same. Since the actual volumetric gas flow rate was at least 62 times that of the liquid volumetric flow rate, the residence time was mainly a function of gas flow rate. Therefore, due to the pressure effect on the actual volumetric flow rate of gas, the residence time increased with the increase in reaction pressure. In addition, the concentration of dissolved H_2 was also positively affected by the pressure increase.

As shown in Figure 5 (a) and (b), the hydrocarbon yield increases with increase in reaction pressure during the 7 hours of reaction, which shows the positive effect of dissolved H_2 concentration and residence time on the activity of precious metal-based catalyst. The initial hydrocarbon yield at 500 psig was all around 60% for Pt, Rh and NiMo [14], however, unlike NiMo catalyst, whose initial catalyst activity was not affected by the reaction pressure [14], the initial activity of Pt and Rh both increased with the reaction pressure. It can be observed that the hydrocarbon yield over Pt and Rh kept decreasing during the first 4 hours run, and then stabilized; however, no stabilized hydrocarbon yield was observed in NiMo results, and the decreasing rate of NiMo activity kept increasing with reaction time-on-stream, which indicated the occurrence of deactivation possibly due to the accumulation of by-products, such as oxygenated intermediates and coke [14]. It is seen that the increase in reaction pressure has a negative effect on the stability of activity of precious metal-based catalysts. It could be due to the difficulty in desorption of product molecules from the catalyst surface at high reaction pressure. Moreover, as mentioned above, due to the Rh initial activity in hydrocracking, which produced substantial amount of CH_4, the hydrogen partial pressure was greatly reduced. As a result, the hydrocarbon yield over Rh decreased much faster during the first 4 hours than for both Pt and NiMo. At 300 psig, the initial hydrocarbon yield over Rh was higher than that over Pt, and then both stabilized around 10% after 4 hours. For the reaction pressure 400 psig and above, the stabilized activity of Pt is higher than that of Rh, and both are higher than the extrapolated stable activity of NiMo.

The ratios of even-numbered carbon hydrocarbon to odd-numbered carbon hydrocarbon at different reaction pressures were all less than 1 for 7 h on stream (Figure 5 (c) and (d)), which confirm that both Pt and Rh prefer the DCO/DCO2 route over the DHYD route. It can also be observed that HC(2n)/HC(2n-1) ratio decreases with reaction pressure, which indicates that the reaction pressure affects both catalyst activity and selectivity to DCO/DCO2 reaction in the same direction. Furthermore, the HC(2n)/HC(2n-1) ratio increases with the on-stream time, which confirms the correlation of catalyst activity with its selectivity.

From the analysis above, it can be concluded that, within the experimental pressure range, higher reaction pressure is needed to obtain a higher hydrocarbon yield with a lower HC(2n)/HC(2n-1) ratio for both Pt and Rh catalyst. As reported previously, hydrogen is not only a reactant but it also serves to protect the catalyst by preventing the adsorption of oxygenated intermediates and coke [14,39]. However, this beneficial effect was found not to be monotonically increasing in the study of model compounds, that is, a decrease of hydrocarbon yield was observed when hydrogen partial pressure was above a certain range, which is in agreement with the previously reported NiMo result [14,39]. It indicates the existence of an optimum hydrogen to oil ratio on the catalyst surface, which could be due to the competitive adsorption of H_2 and algae oil molecules on the catalyst surface [40]. A detailed kinetic study is needed to verify this hypothesis.

3.7. Effect of Reaction Temperature

Experiments were carried out in the temperature range of 280 ^{o}C to 360 ^{o}C to investigate the temperature effect on catalyst activity and selectivity. Reaction pressure, H_2/Oil ratio, fluid flow rates and weight hourly space velocity (WHSV) were kept the same. It should be noted that despite the temperature effect on the actual volumetric gas flow rate, the residence time varied between a narrow ranges, 0.92s to 1.05s, and was not considered as a factor in the analysis of product yield and product distribution results as shown in Figure 6.

Figure 6 (a) and (b) show that the hydrocarbon yield increases with increase in reaction temperature over both Pt and Rh catalyst, and similar temperature effect was also obtained from NiMo catalyst [14]. Also, at elevated temperatures, the three catalysts all lost their activity with time at a moderate rate. As was reported previously, this beneficial effect from increase in reaction temperature could be explained by the Arrhenius theory of the dependence of reaction rates on temperature. Moreover, the increase in temperature will effectively lower the viscosity of the liquid feed, and enhance the gas-liquid mass transfer, which will result in increased concentration of dissolved H_2 [41]. At 360 ^{o}C, the C13 to C20 hydrocarbon yield over all three catalysts was shown to be high, and increased following the order: Pt > NiMo [14] > Rh. There was no sign of reduction in NiMo activity for at least 7 hours, however, slight decrease in Pt and Rh activity was observed which indicates that the mechanism of deactivation of Pt and Rh is different from that of NiMo. The rate of decrease of Rh activity was much smaller at elevated temperature, which indicates that reduction in activity caused by H_2 partial pressure reduction could be mitigated by elevating reaction temperature. It should be mentioned that the cracking of biofuel molecules over different catalysts may occur at different temperatures, with Rh having the lowest cracking temperature of the three studied catalysts. The light hydrocarbons (less than 13 carbons) that were produced from hydrocracking over Rh was not accounted for in this comparison. The yield of hydrocracking product was found to also increase with the reaction temperature, which decreased the C13 to C20 hydrocarbon yield over Rh. Moreover, it would also decrease the hydrocarbon yield increase per degree of reaction temperature increase, which weakened the apparent temperature effect on the improvement of Rh activity. At 280 ^{o}C, Rh showed the highest initial activity among the three investigated catalysts, and after 4 hours, the lowest stabilized hydrocarbon yield was obtained over NiMo. For reaction temperature between 360 ^{o}C and 280 ^{o}C, hydrocarbon yield over precious metal decreased during the first 4 hours run, and then stabilized, however, again no stability could be reached over NiMo within 7 hours run. By examining the trend of hydrocarbon yield with time, it is expected that, the stabilized C13 to C20 hydrocarbon yield should decrease following the order: NiMo< Rh< Pt.

As shown in Figure 6 (c) and (d), the HC(2n)/HC(2n-1) ratio over Rh was slightly smaller than that of Pt at the same temperature. This ratio decreases with increase of reaction temperature, but at different rates, which reflect the increase of the Pt and Rh selectivity to DCO/DCO2 reaction with reaction temperature. However, as reported previously, the selectivity of NiMo was less sensitive to temperature at 310 ^{o}C and above [14]. It can also be concluded that the HC(2n)/HC(2n-1) ratio tends to be more stable at elevated temperatures, which again confirms the correlation between activity and selectivity for precious metal-based catalysts when varying the operating temperature.

3.8. Effect of Hydrogen to Oil Ratio

Hydrogen to oil ratio (H_2/Oil) is as an important process parameter in the upgrading of algae oil via HDO. It represents the ratio of hydrogen feed (sccm, standard cubic centimeter per minute) to the total liquid feed (mL/min, solvent included). In the present work, five H_2/Oil ratios ranging between 385 SmL/mL and 1000 SmL/mL were studied by varying the liquid flow rate at the same gas flow rate. Therefore, residence time was kept constant at different H_2/Oil ratios. Since catalyst loading remained the same for all runs, WHSV was reduced when increasing H_2/Oil ratio.

As depicted in Figure 7 (a) and (b), the hydrocarbon yield over all three studied catalyst was found to increase with the increase of H_2/Oil ratio. This could be explained by the enhancement of the gas-liquid convective mass transfer, which is a strong function of the liquid slug length [42]. In addition, it has been reported that the increase in H_2/Oil ratio can effectively decrease the formation of oligomerized product (> C18) and cracked products, which can lead to the increase in the yield of C13-C18 hydrocarbons [43]. The initial activity of NiMo is more sensitive to H_2/Oil ratio than that of the studied precious metal-based catalysts [14]. Moreover, for H_2/Oil ratio of 715 SmL/mL and below, the initial activity of Pt and Rh was hindered by the insufficient mass transfer, and this inhibition on NiMo was found to occur at an even lower H_2/Oil ratio. This could be due to the high active site density of the NiMo catalyst. With time, the activity of Rh was found to decrease much faster than that of Pt during the first 4 hours, and it could be caused by the reduction of H_2 partial pressure due to the production of CH_4. After reaching stability, the activity was positively affected by the H_2/Oil ratio; moreover, the stabilized hydrocarbon yield was about the same for NiMo, Pt and Rh. At H_2/Oil ratio of 1000 SmL/mL, the stabilized hydrocarbon yield over Pt is higher than the Rh, however, no stability was reached over NiMo within 7 hours reaction and its decreasing rate was increasing with reaction time-on-stream [14].

The H_2/Oil ratio had the greatest effect on the initial selectivity of NiMo, and the least on Pt. The ratio of HC(2n)/HC(2n-1) (Figure 7 (c) and (d)) over Pt and Rh is less than 1 although it changes with time during the 7-hour reaction, which reflects primarily a selectivity to DCO/DCO2 route. However, the HC(2n)/HC(2n-1) ratio over NiMo was found to be less than 1 for H_2/Oil less than 1000 SmL/mL after 4 hours of reaction, which shows that the selectivity of NiMo was affected by the H_2/Oil ratio and time-on-stream [14]. The stability of the Pt and Rh activity seemed to be negatively affected by the H_2/Oil ratio. For the H_2/Oil ratio less than 715 SmL/mL, the selectivity of both Pt and Rh was not affected by the H_2/Oil ratio and was stable for at least 7 hours, with Pt giving a slightly lower H(2n)/HC(2n-1) ratio; however, for the ratio above 715 SmL/mL, the H_2/Oil effects on the selectivity of Pt and Rh were opposite; the higher the H_2/Oil ratio was, the lower the H(2n)/HC(2n-1) ratio for Rh, but the higher for Pt.

3.9. Effect of Residence Time

Residence time is an indication of the average time that the reactants spend inside the reactor. It can be calculated by dividing the volume of the reactor with the total superficial volumetric flow rates of the reactants based on the empty bed assumption. In this study, the residence time was adjusted by varying the reactor length while keeping the gas and liquid flow rate constant. Since the catalyst loading was increased with the increase of reactor length, the WHSV decreased with the increase of residence time. Reactor ID was kept the same for all runs, therefore, the flow velocity was help constant and the convective mass transfer would not affect the reactor performance results in this set of experiments.

The results summarized in Figure 8 (a) and (b) show that the catalyst activity and its stability both increase with increase in residence time. The same phenomenon was observed when studying the NiMo catalyst [14]. At the same residence time, the catalyst stability increases in the following order: Pt > Rh > NiMo. For residence time 1s and above, the hydrocarbon yield over Pt and Rh stabilized, and the stabilized hydrocarbon yield over Pt was higher than that of Rh. However, no stability was reached over NiMo within 7 hours. The prolongation of residence time over Rh and Pt effectively helped to maintain the catalysts activity. At residence time of 1.5s, there was no sign of reduction in the hydrocarbon yield over Pt for at least 7 hours. For residence time less than 1s, the hydrocarbon yield stabilized around the same value over the three catalysts. The residence time effect on HC(2n)/HC(2n-1) ratio over Pt and Rh is depicted in Figure 8 (c) and (d). At the residence time less than 1s, the HC(2n)/HC(2n-1) ratio was reported to change over NiMo with residence time, but the selectivity of Pt and Rh was not affected. For the residence time below 1.5s, unlike the NiMo results [14], the HC(2n)/HC(2n-1) ratio over Pt and Rh was not affected by the residence time increase, but all stabilized around the same value.

The lowest ratio was obtained at the longest residence time, whereas for NiMo, it was the highest ratio as reported in [14]. The improved performance obtained at higher residence time could be due to the reduction of WHSV, which indicates that per unit mass, the catalyst is exposed to less amount of feedstock. Although no further increase in residence time is needed in the present reactor system for the hydrotreating of microalgae oil, it is still necessary to point out that increase in residence time can possibly lead to the decrease in desired diesel range products due to the increase in secondary reactions of hydrocarbons, such as cracking and oligomerization [44].

4. Conclusions

Green diesel production from microalgae (Nannochloropsis salina) oil via hydrodeoxygenation has been investigated over 1% Pt/Al_2O_3, 0.5% Rh/Al_2O_3 and presulfided NiMo/Al_2O_3 catalysts in a microreactor. Coke accumulation decreased in the order NiMo > Pt > Rh, and the amount of coke formed over NiMo increased with reaction duration, while no on-stream time dependence was found over Pt and Rh. Platinum and Rhodium were both active for CH_4 formation at their fresh reduced state, with Rh giving the highest CH_4 yield and Pt having the longest (> 30 hours) CH_4 formation activity; but no detectable amount of CH_4 was formed over NiMo during the reaction. As on-stream-time increases, the formation of CH4 over Pt and Rh both decreased, and no methane was produced after the reaction reached stability. Methane was mainly produced through hydrocracking initially, and then via methanation, which was confirmed by the liquid product analysis and the hydrogen consumption results. The stabilized hydrogen consumption over the three investigated catalysts decreased following NiMo > Pt > Rh, which confirms that the DHYD route demands more hydrogen than DCO/DCO2 route in removing the same amount of oxygen. Comparing the measured H_2 consumption with the theoretical H_2 demand based on the identified FA in the feedstock, it can be concluded that the HDO mechanism of unidentified portion of the algae oil is different from that of FA.

After investigating the susceptibility to coking, disposition towards methane formation, and hydrogen consumption of each catalyst, on the basis of external and internal mass transfer analysis, performance study was conducted to evaluate the activity and selectivity of these three catalysts by studying changes in the yield and distribution of diesel-ranged alkanes as a function of operating parameters, namely reaction temperature, pressure, hydrogen to oil ratio and residence time. The results reveal that the Pt and Rh favor the DCO/DCO2 route and their selectivity was not affected by the experimental conditions; however, the selectivity of NiMo was changed from DHYD to DCO/DCO2 at reduced H_2/Oil ratio and residence time. The HC(2n)/HC(2n-1) ratio over Pt and Rh was more sensitive to temperature than over NiMo. The activity and selectivity of all three investigated catalysts were positively affected by elevating reaction pressure, temperature, H_2/Oil ratio and residence time. Under these conditions, the hydrocarbon yield over Pt and Rh was found to be stabilized after 4 hours of reaction, but no stability was reached over NiMo within 7 hours. It is reasonable to extrapolate that the activity of Pt and Rh catalyst will be maintained for longer on-stream time at elevated operating conditions. Moreover, the NiMo activity decreases with time on stream, indicating the occurrence of deactivation, possibly due to the accumulation of by-products. At the highest reaction temperature, 360 ^{o}C, although the activity of Pt and Rh was shown to be high, but slight decrease was observed with time-on-stream, which indicates that the mechanism of deactivation of Pt and Rh was different from that of NiMo.

The formation of CH_4 reduced the H_2 partial pressure and caused the fast decrease of Rh activity initially. However, it can be mitigated by increasing the reaction temperature and the catalyst loading, which will increase the residence time and decrease the WHSV. It should also be noted that the cracking product over Rh was not accounted for in the hydrocarbon yield results, but its amount increases with increasing reaction temperature, which indicates that the oxygen removal efficiency was not fully reflected by only looking at the C13 to C20 hydrocarbon yield. The highest hydrocarbon yield, 76.5%, was obtained over 1% Pt at 310 ^{o}C, 500 psig, H_2/Oil ratio of 1000 SmL/mL and residence time of 1.5 s. Under this condition, the HC(2n)/HC(2n-1) ratio was below 0.3 and both the catalyst activity and selectivity could be maintained for at least 7 hours. Compared with the best performance results of 62.7%, obtained over NiMo catalyst at 360^{o}C and residence time of 1s, the reaction temperature was decreased by 50 ^{o}C with 0.5s increase of residence time from 1 second, which could potentially result in substantial energy saving.

Based on our experience in catalytic hydrotreating of microalgae oil, we found three major challenges that need to be addressed to render the algae to biofuel process economically feasible. The growth and cultivation of microalgae, as measured by the algae area productivity and oil content, represent by far the biggest cost factor. Genetic engineering appears to be a promising approach to increasing both parameters which will provide a path to the production of low-cost feedstock. The development of more cost-effective catalysts that can be commercially used in hydrotreating high concentration algae oils for an extended period of on-stream time without significant deactivation will also contribute to cost reduction. The results of the present study provide guidance on future work in this direction. Loss of catalyst activity will eventually occur, especially with high algae oil concentration feedstocks, therefore an effective catalyst regeneration process needs to be developed to recover activity lost due to coke formation, impurities in the feed solution or adsorption of oxygenates on active catalyst sites.

Acknowledgements

The financial support by the DOE-Bioenergy Technologies Office through grant DE-EE0006063 is gratefully acknowledged. The authors appreciate the support of our principal industrial partner Valicor Renewables LLC, and we are especially grateful to Dr. Brian Goodall for his technical contributions to the study. Special thanks to Dr. James Manganaro for his inspiring guidance, and the painstaking review of the experimental results as well as the manuscript. The authors, of course, bear the sole responsibility for any errors.

References

[1] E.N. Parekh, Pipeline and Gas Journal 240 (2013).
[2] U.S.E.I. Administration. http://www.eia.gov/energyexplained/index.cfm?page=diesel_home. Last accessed May 5, 2015.
[3] E. Facts, US EPA. http://www.chargepoint.com/files/420f05001.pdf. Last accessed May 5, 2015.
[4] J.A. Melero, J. Iglesias, A. Garcia, Energy & Environmental Science 5 (2012) 7393-7420.
[5] L. Brennan, P. Owende, Renewable and Sustainable Energy Reviews 14 (2010) 557-577.
[6] B. Peng, Y. Yao, C. Zhao, J.A. Lercher, Angewandte Chemie 124 (2012) 2114-2117.
[7] D. Kubička, J. Horáček, Applied Catalysis A: General 394 (2011) 9-17.
[8] B. Donnis, R.G. Egeberg, P. Blom, K.G. Knudsen, Topics in Catalysis 52 (2009) 229-240.
[9] J. Holmgren, C. Gosling, K. Couch, T. Kalnes, T. Marker, M. McCall, R. Marinangeli, Petroleum Technology Quarterly 12 (2007) 119.
[10] J. Holmgren, C. Gosling, R. Marinangeli, T. Marker, G. Faraci, C. Perego, Hydrocarbon Processing 86 (2007) 67-72.
[11] E. Laurent, B. Delmon, Applied Catalysis A: General 109 (1994) 77-96.
[12] E. Laurent, B. Delmon, Applied Catalysis A: General 109 (1994) 97-115.
[13] P. Šimáček, D. Kubička, G. Šebor, M. Pospíšil, Fuel 88 (2009) 456-460.
[14] L. Zhou, A. Lawal, Energy & Fuels 29 (2015) 262-272.
[15] O. Şenol, T.-R. Viljava, A. Krause, Catalysis Today 100 (2005) 331-335.

[16] O.I. Senol, T. Viljava, A. Krause, Catalysis Today 106 (2005) 186-189.

[17] A. Bridgwater, Applied Catalysis A: General 116 (1994) 5-47.

[18] O. Şenol, E.-M. Ryymin, T.-R. Viljava, A. Krause, Journal of Molecular Catalysis A: Chemical 277 (2007) 107-112.

[19] O. Şenol, T.-R. Viljava, A. Krause, Applied Catalysis A: General 326 (2007) 236-244.

[20] K.O. Albrecht, R.T. Hallen, A Brief Literature Overview of Various Routes to Biorenewable Fuels from Lipids for the National Alliance for Advanced Biofuels and Bio-products (NAABB) Consortium, Pacific Northwest National Laboratory Richland, WA, 2011.

[21] P. Mäki-Arvela, M. Snåre, K. Eränen, J. Myllyoja, D.Y. Murzin, Fuel 87 (2008) 3543-3549.

[22] V. DUNDICH, V. YAKOVLEV. Chemistry for Substainable Development 17 (2009) 521-526.

[23] I. Kubičková, M. Snåre, K. Eränen, P. Mäki-Arvela, D.Y. Murzin, Catalysis Today 106 (2005) 197-200.

[24] A.T. Madsen, C.H. Christensen, R. Fehrmann, A. Riisager, Fuel 90 (2011) 3433-3438.

[25] N. Joshi, A. Lawal, Chemical Engineering Science 74 (2012) 1-8.

[26] N. Joshi, A. Lawal, Chemical Engineering Science 84 (2012) 761-771.

[27] N. Joshi, A. Lawal, Industrial & Engineering Chemistry Research 52 (2013) 4049-4058.

[28] D. Qian, A. Lawal, Chemical Engineering Science 61 (2006) 7609-7625.

[29] S. Tadepalli, R. Halder, A. Lawal, Chemical Engineering Science 62 (2007) 2663-2678.

[30] S. Tadepalli, D. Qian, A. Lawal, Catalysis Today 125 (2007) 64-73.

[31] M.A. Halabi, A. Stanislaus, A. Qamra, S. Chopra, Studies in Surface Science and catalysis 100 (1996) 243-251.

[32] Fogler, H.S., 2005. Elements of Chemical Reaction Engineering, fourth ed. Prentice Hall Professional Technical Reference. pp. 839-841.

[33] M.A. Matthews, J.B. Rodden, A. Akgerman, Journal of Chemical and Engineering Data 32 (1987) 319-322.

[34] J. Edvardsson, P. Rautanen, A. Littorin, M. Larsson, Journal of the American Oil Chemists' Society 78 (2001) 319-327.

[35] R. Egeberg, N. Michaelsen, L. Skyum, Novel hydrotreating technology for production of green diesel. Lyngby, Denmark: Haldor Topsoe A/S, 2012. pp. 3.

[36] Houghton, John Theodore, Y. D. J. G. Ding, David J. Griggs, Maria Noguer, Paul J. van der Linden, Xiaosu Dai, Kathy Maskell, and C. A. Johnson. "Climate change 2001: the scientific basis." (2001). [37] P.T. Do, M. Chiappero, L.L. Lobban, D.E. Resasco, Catalysis Letters 130 (2009) 9-18.

[38] D. Kubička, L. Kaluža, Applied Catalysis A: General 372 (2010) 199-208.

[39] Mäki-Arvela, Päivi, et al. "Catalytic deoxygenation of fatty acids and their derivatives." *Energy & Fuels* 21.1 (2007): 30-41.

[40] Boda, László, et al. "Catalytic hydroconversion of tricaprylin and caprylic acid as model reaction for biofuel production from triglycerides." *Applied Catalysis A: General* 374.1 (2010): 158-169.

[41] Ayodele, Olumide Bolarinwa, Hazzim F. Abbas, and Wan Mohd Ashri Wan Daud. "Hydrodeoxygenation of stearic acid into normal and iso-octadecane biofuel with zeolite supported palladium-oxalate catalyst." *Energy & Fuels* 28.9 (2014): 5872-5881.

[42] M.T. Kreutzer, P. Du, J.J. Heiszwolf, F. Kapteijn, J.A. Moulijn, Chemical Engineering Science 56 (2001) 6015-6023.

[43] Anand, Mohit, and Anil K. Sinha. "Temperature-dependent reaction pathways for the anomalous hydrocracking of triglycerides in the presence of sulfided Co–Mo-catalyst." *Bioresource technology* 126 (2012): 148-155.

[44] Yang, Yuhan, et al. "Hydrotreating of C 18 fatty acids to hydrocarbons on sulphided NiW/SiO 2–Al 2 O 3." *Fuel Processing Technology* 116 (2013): 165-174.

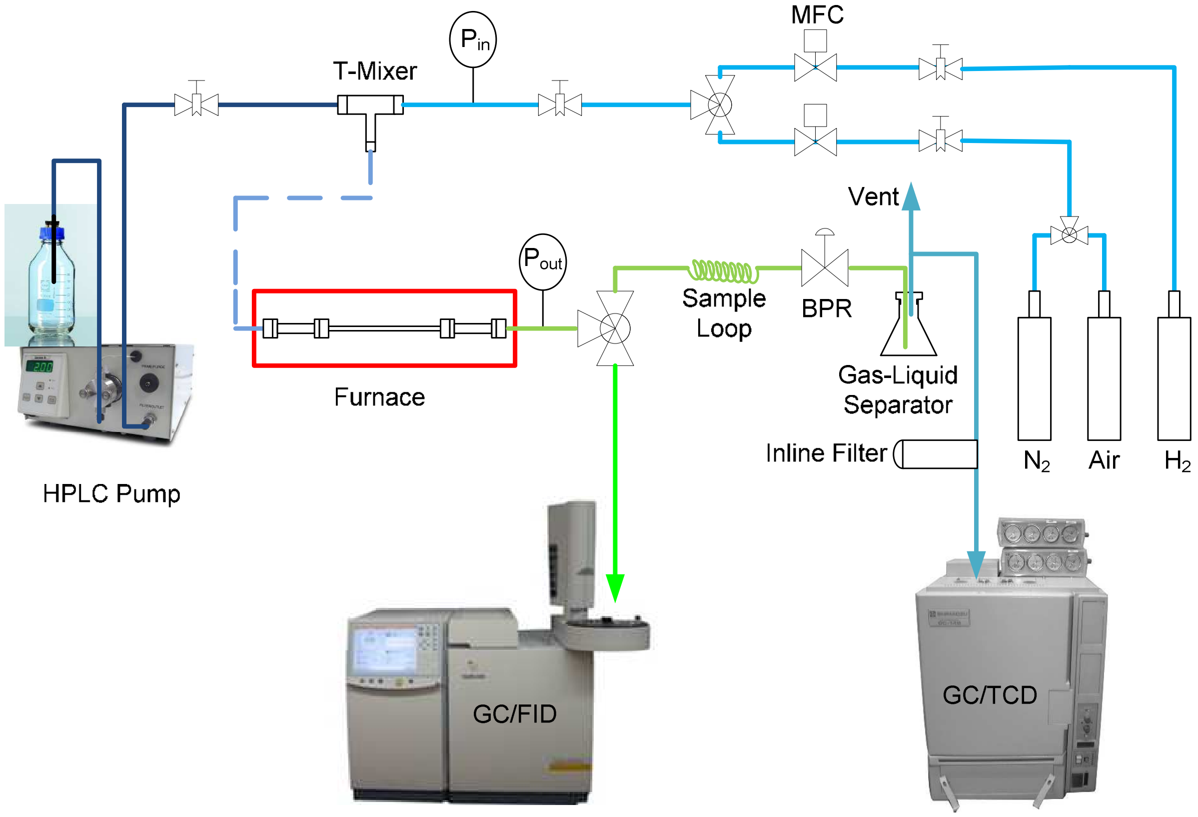

Scheme 1. Schematic of Microalgae Oil Hydrodeoxygenation Setup

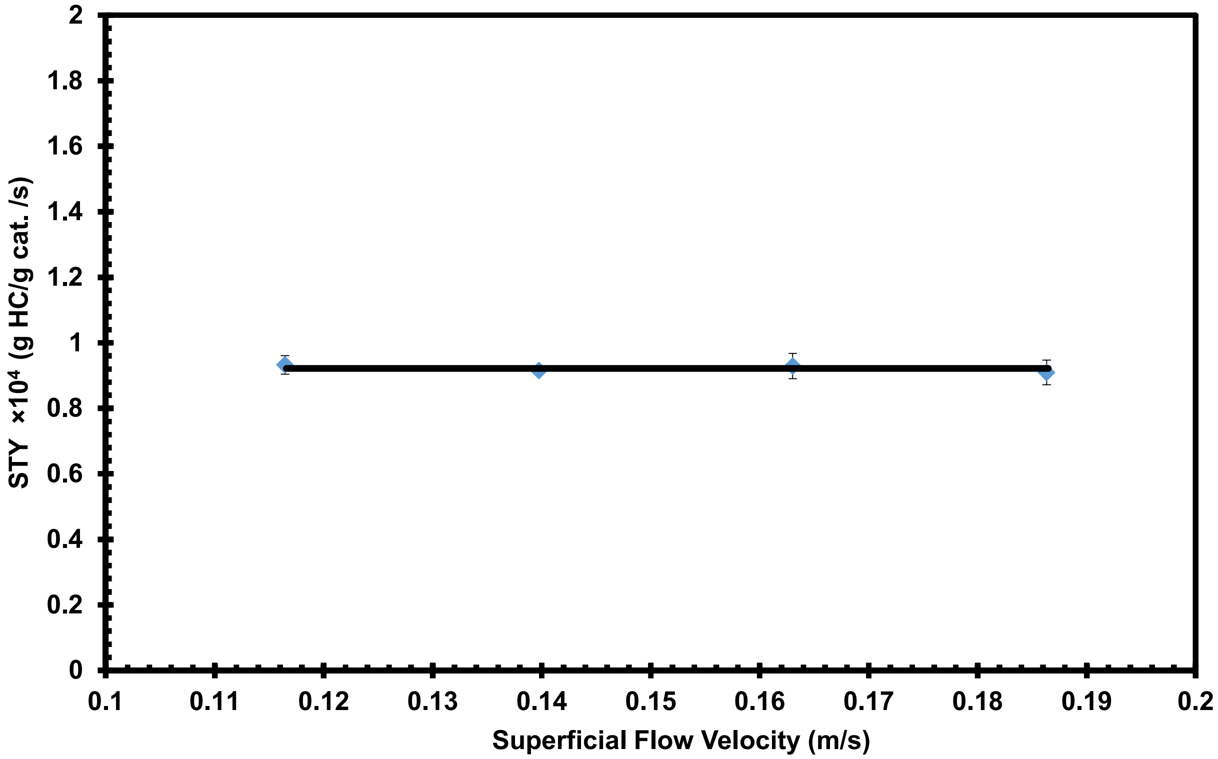

Figure 1. Effect of superficial flow velocity on space-time yield of C13 to C20 hydrocarbon. (1% Pt, 1.32 wt % Nannochloropsis salina oil in dodecane, Temperature = 310 °C, H_2 pressure = 500 psig, Residence time = 1 s, H_2/oil = 1000 SmL/mL).

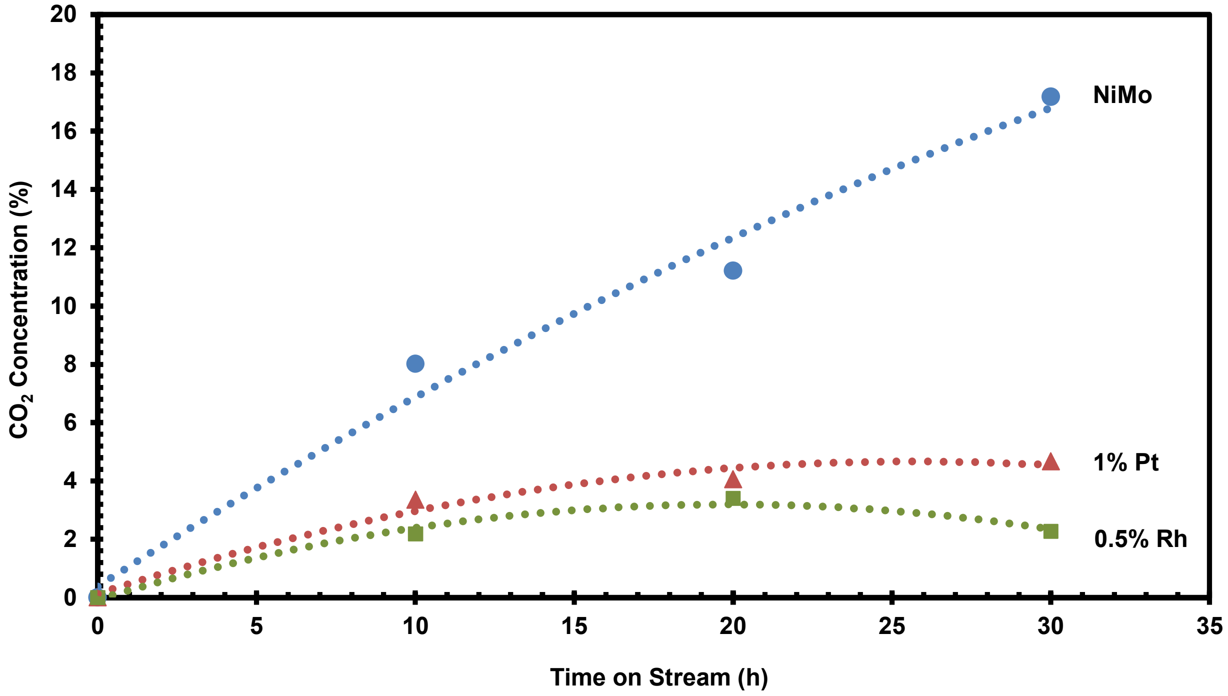

Figure 2: CO_2 concentration in combustion product gas (Reaction: 80mg catalyst, 1.32 wt% Nannochloropsis salina oil in dodecane, 0.05ml/min, Temperature=360 ^{o}C, H_2 pressure=500 psig, H_2/Oil=100 Sml/ml; Combustion: 5sccm Air, 650 ^{o}C.)

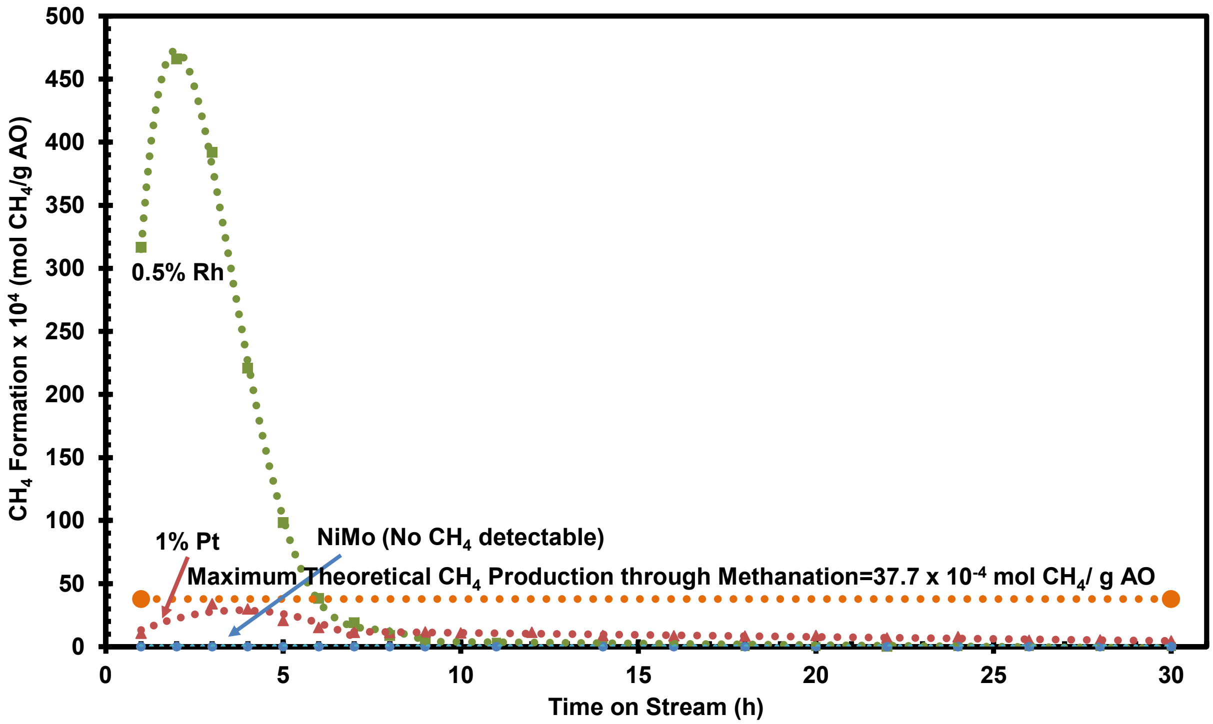

Figure 3: CH_4 formation per gram microalgae oil processed (80mg catalyst, 1.32wt% Nannochloropsis salina oil in dodecane, 0.05ml/min, Temperature=360°C, Reaction pressure=500 psig, H_2 flow rate=4 sccm, N_2 flow rate=1 sccm).

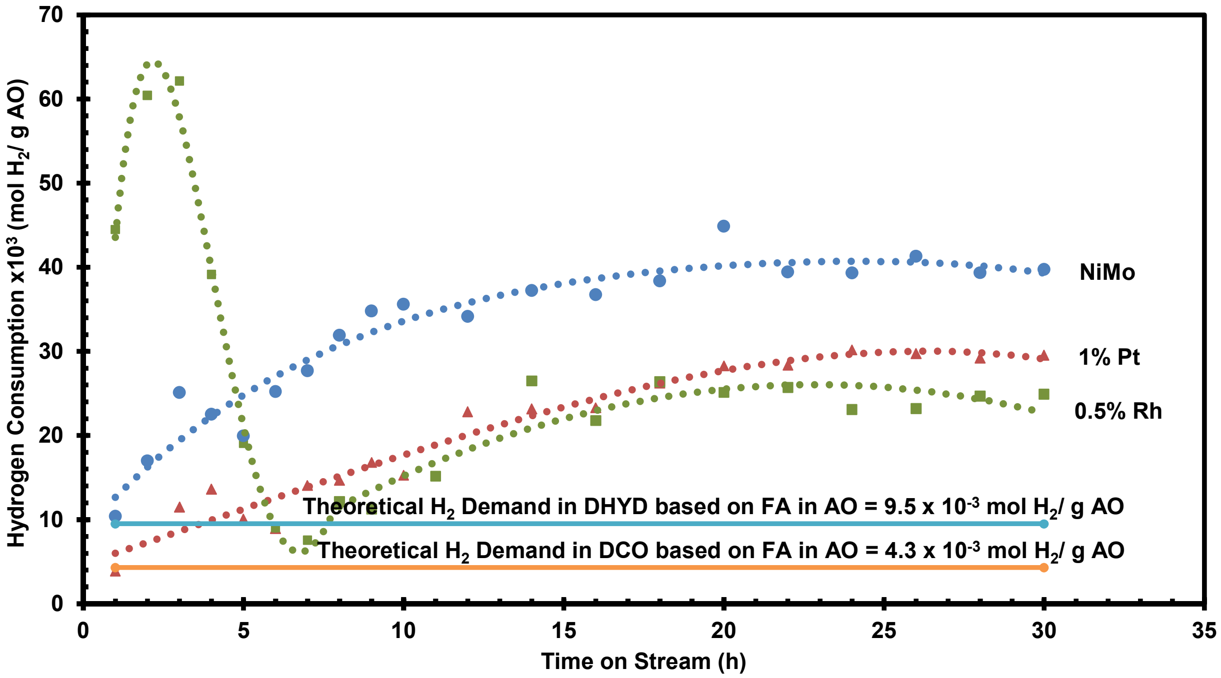

Figure 4. Hydrogen consumption (80mg catalyst, 1.32wt% Nannochloropsis salina oil in dodecane, 0.05ml/min, Temperature=360°C, Reaction pressure=500 psig, H_2 flow rate=4 sccm, N_2 flow rate=1 sccm).

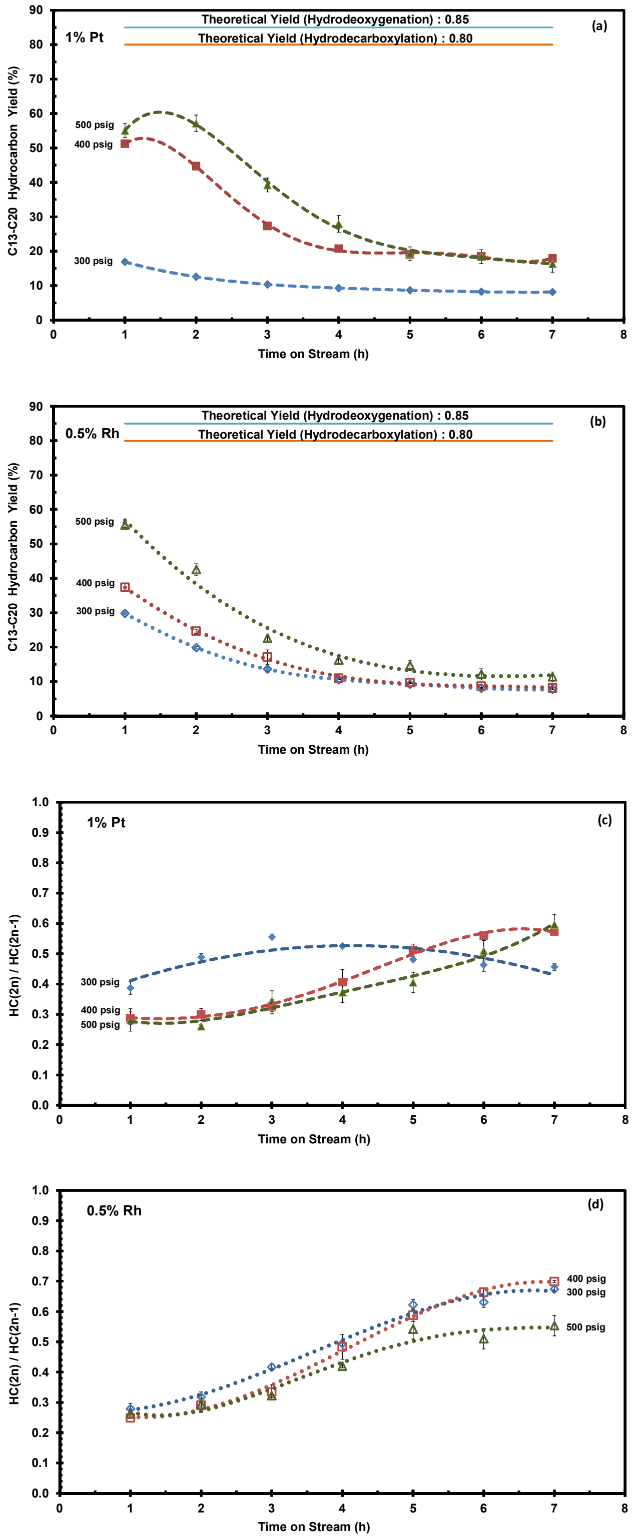

Figure 5. Effect of reaction pressure on C13 to C20 hydrocarbon yield: (a) 1% Pt, (b) 0.5% Rh; ratio of even-numbered carbon hydrocarbon to odd-numbered carbon hydrocarbon: (c) 1% Pt, (d) 0.5% Rh (60mg catalyst, 1.32 wt % Nannochloropsis salina oil in dodecane, Temperature = 310 °C, WHSV = 0.65 g of oil/g of cat./h).

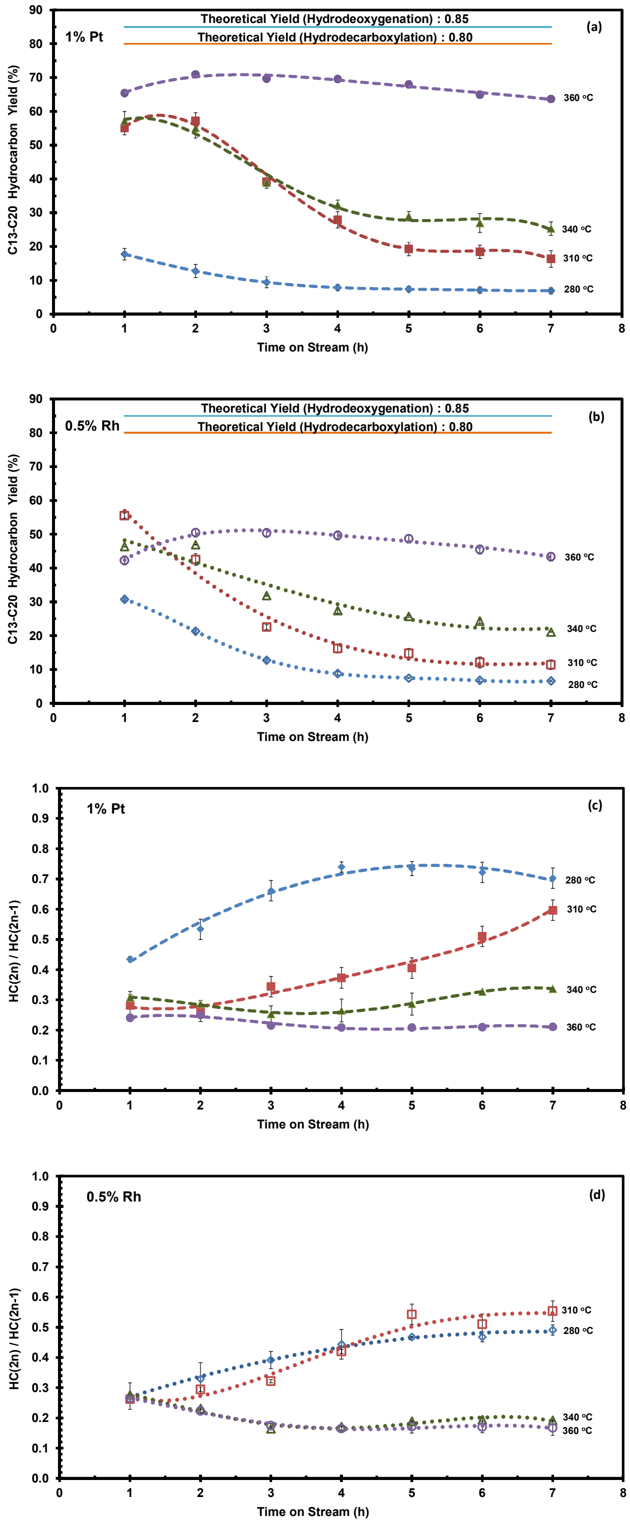

Figure 6. Effect of reaction temperature on C13 to C20 hydrocarbon yield: (a) 1% Pt, (b) 0.5% Rh; ratio of even-numbered carbon hydrocarbon to odd-numbered carbon hydrocarbon: (c) 1% Pt, (d) 0.5% Rh (60mg catalyst, 1.32 wt % Nannochloropsis salina oil in dodecane, H_2 pressure = 500 psig, WHSV = 0.65 g of oil/g of cat. /h).

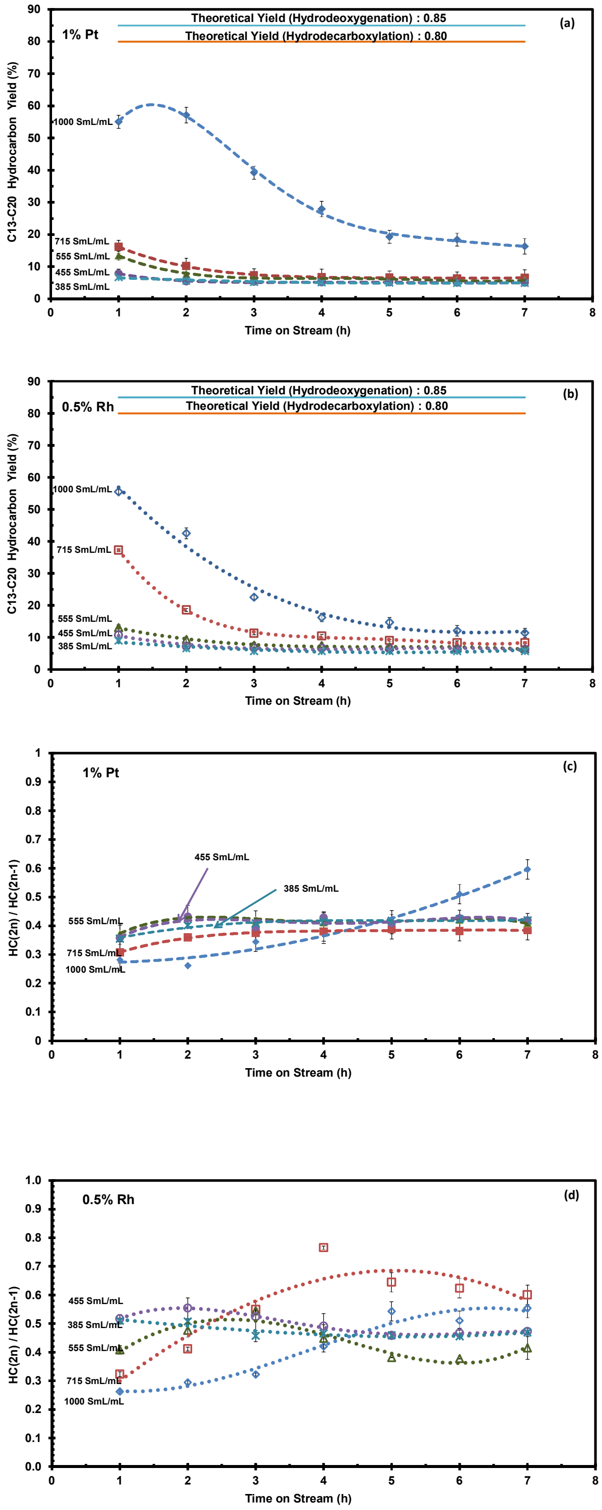

Figure 7. Effect of H_2/oil ratio on C13 to C20 hydrocarbon yield: (a) 1% Pt, (b) 0.5% Rh; ratio of even-numbered carbon hydrocarbon to odd-numbered carbon hydrocarbon: (c) 1% Pt, (d) 0.5% Rh (60mg catalyst, 1.32 wt % Nannochloropsis salina oil in dodecane, Temperature = 310 °C, H_2 pressure = 500 psig, Residence time = 1s, GHSV = 55000 h^{-1}).

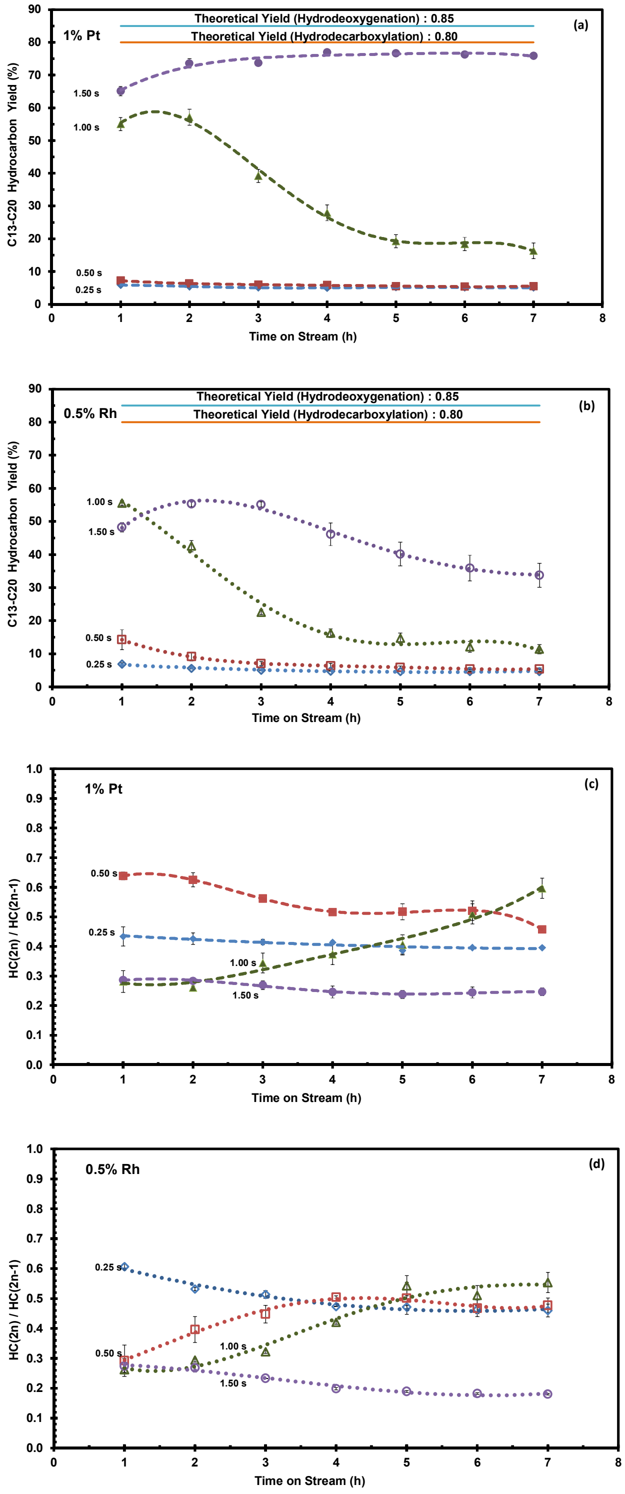

Figure 8. Effect of residence time on C13 to C20 hydrocarbon yield: (a) 1% Pt, (b) 0.5% Rh; ratio of even-numbered carbon hydrocarbon to odd-numbered carbon hydrocarbon: (c) 1% Pt, (d) 0.5% Rh (1.32 wt % Nannochloropsis salina oil in dodecane, Temperature = 310 °C, H_2 pressure = 500 psig, Superficial flow velocity = 0.117 m/s).

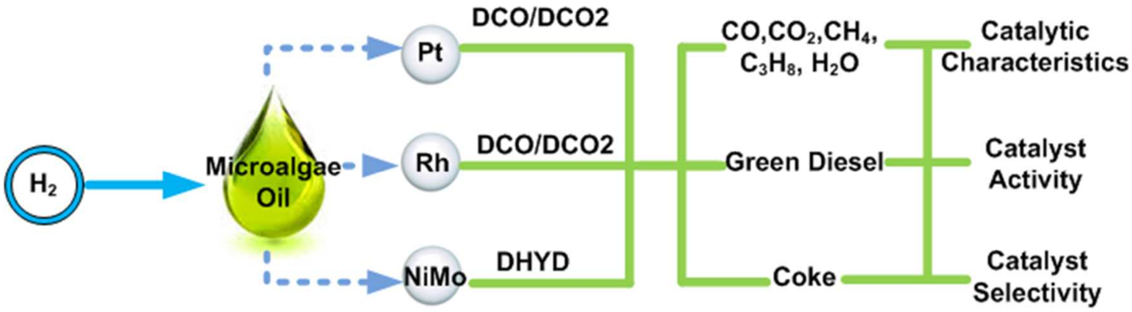
H$_2$
Microalgae Oil
Pt
Rh
NiMo
DCO/DCO2
DCO/DCO2
DHYD
CO,CO$_2$,CH$_4$, C$_3$H$_8$, H$_2$O
Green Diesel
Coke
Catalytic Characteristics
Catalyst Activity
Catalyst Selectivity